Electronic supplementary information for

Uncovering a Law of Corresponding States for Electron Tunneling in Molecular Junctions

Ioan Bâldea[1,*], Zuoti Xie[2] , and C. Daniel Frisbie[2]

[1]Theoretische Chemie, Universität Heidelberg, INF 229, 69120 Heidelberg, Germany

[2]Department of Chemical Engineering and Materials Science, University of Minnesota, Minneapolis, Minnesota 55455, USA

Corresponding authors: ioan.baldea@pci.uni-heidelberg.de (I.B.), zxie@umn.edu (Z.X.); frisbie@umn.edu (C.D.F.)

*Also at ISS-NILPRP RO 0077125, Bucharest-Măgurele, Romania

Supplementary text

Cross-over voltage versus transition voltage. The voltage V_c at the maximum of the curve $|V^2/I|$ *vs.* V (Fig. 1 in the main text and Fig. S7 below) represents an alternative equivalent term proposed here to the so-called transition voltage (V_t) introduced in Ref. 16 cited in the main text as the minimum of the so-called Fowler-Nordheim quantity ln $|I/V^2|$. We prefer to use V_c instead of V_t, because the term "transition" associated with the latter may be (mis)interpreted as a change between two different transport mechanisms, which is not the case. The term "cross-over" used here is related a feature that can be directly extracted by recasting measured *I-V* curves (Fig. 1a in the main text and Fig. S7a below) in coordinates $|V^2/I|$ *vs.* V (Fig. 1b and S7b). As explained below, this cross-over is the result of a nearly linear dependence I vs. V at lower biases, which gradually becomes more super-linear at higher biases. Let us consider the range $V>0$ ($I>0$). The almost linear increase ($I \propto V$) at low V yields a nearly linear increase of the quantity V^2/I with increasing V (biases $V<V_c$ in Fig. S7b). At higher biases, the current I increases faster than V^2, so

that the ratio V^2/I decreases with increasing V (biases $V>V_c$ in Fig. S7b). As it increases at lower biases and decreases at higher biases, the quantity V^2/I should necessarily possess a maximum, which defines the cross-over bias V_c.

Measurement errors versus statistical errors. In addition to the statistical errors shown in Fig. 2c of the main text and in Fig. S1 to S6, we present below (Fig. S8 to S10) what we call "measurement errors"; their meaning can be understood by inspecting Fig. S7. It is worth emphasizing that, in contrast to statistical errors, which refer to statistical ensembles comprising many traces, these measurement errors refer to a single I-V trace and are due to uncertainties in identifying the exact location of the maximum of the quantity $V^2/|I|$ (cf. Fig. S7).

Additional figures

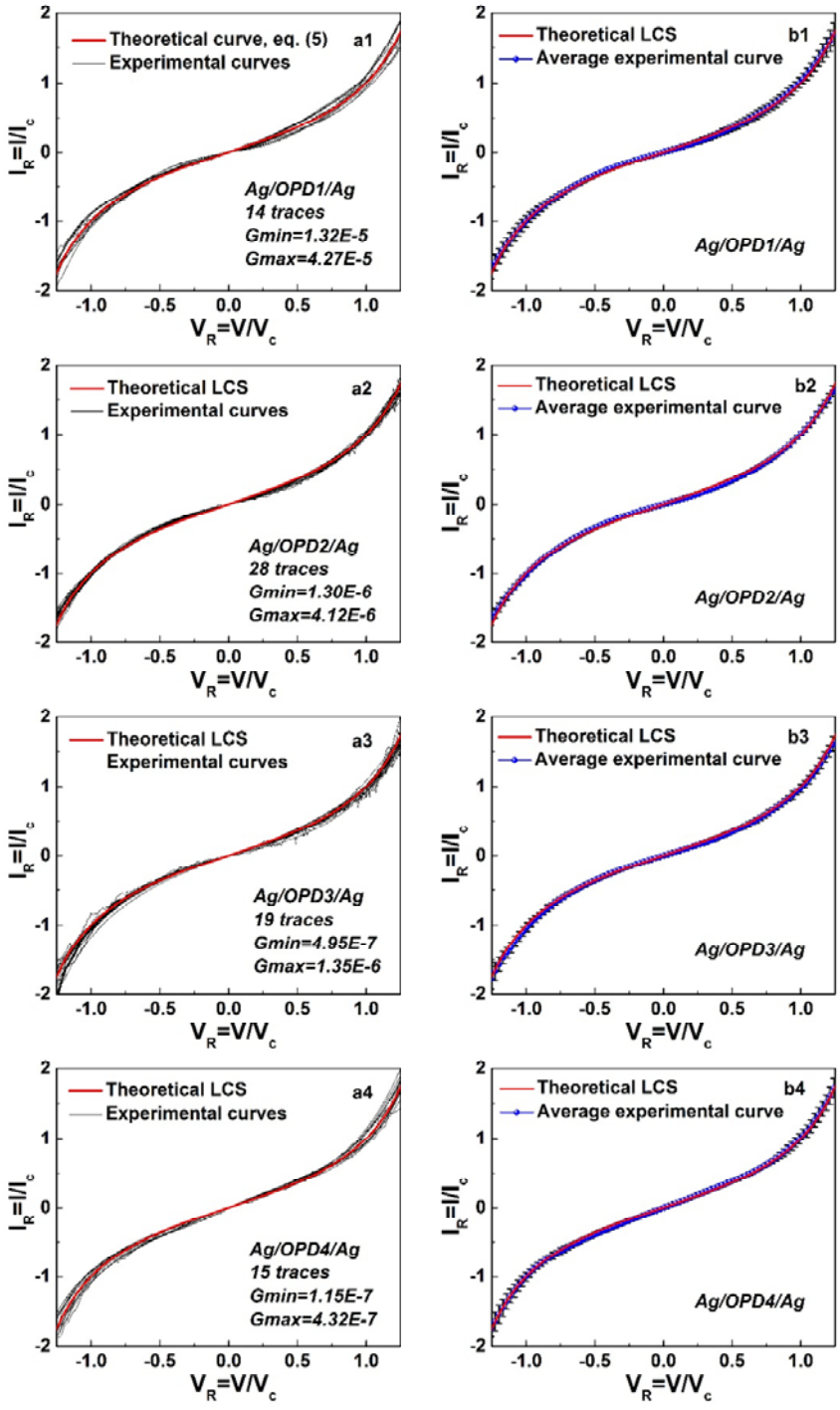

Fig. S1. Current-voltage curves in reduced variables for Ag/OPDn/Ag CP-AFM junctions. (a) The theoretical curve (red) given by eqn (6) plotted along with the experimental curves (black) measured for different types of oligophenylene dithiol species (n=1 to 4). (b) Comparison of the theoretical (red) curve and the ensemble average (blue line) of the experimental curves. Error bars (black) represent standard statistical deviations. The number of traces as well as the minimum and maximum values of the low-bias conductance *G* are given in legends.

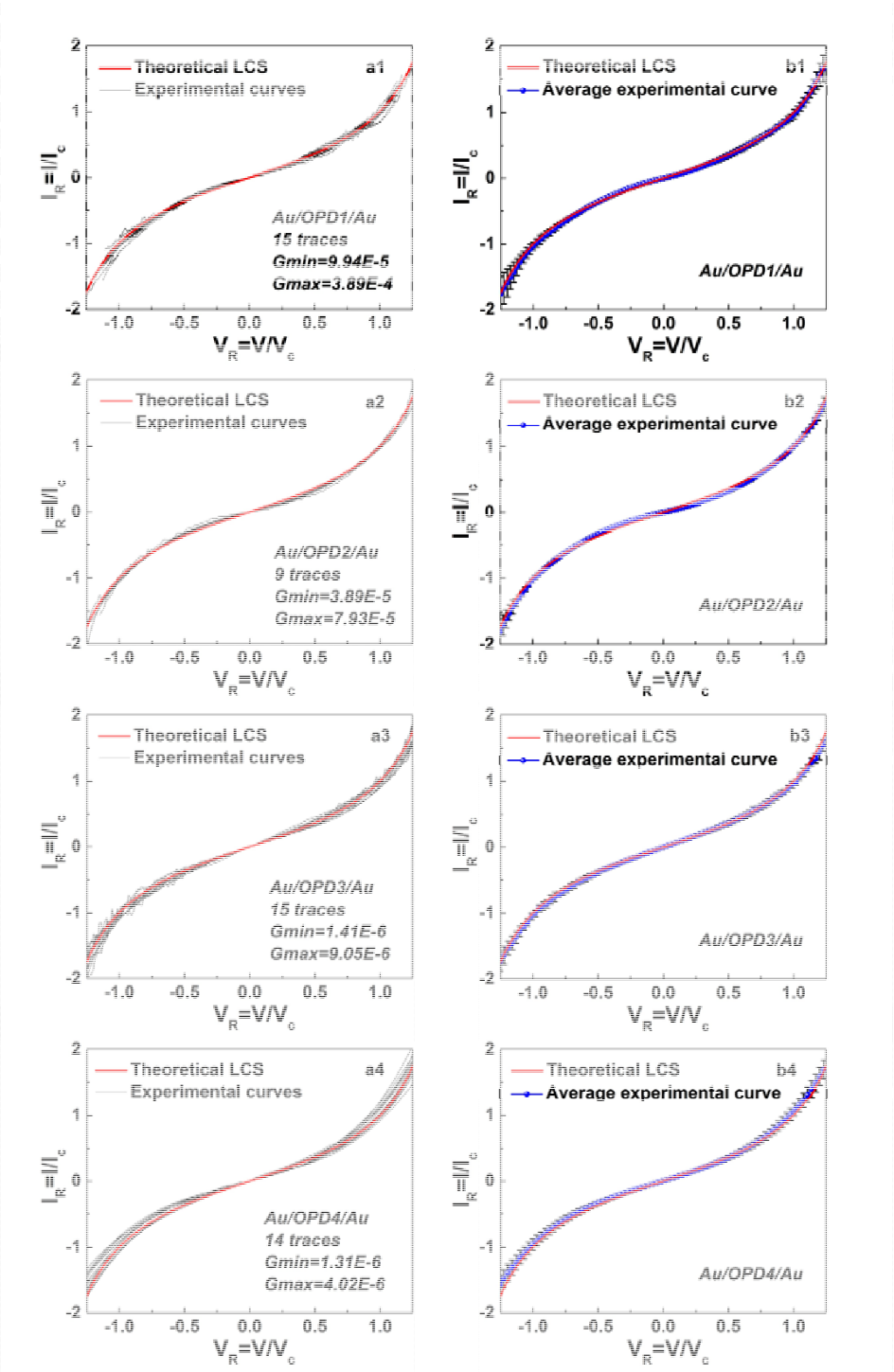

Fig. S2. Current-voltage curves in reduced variables for Au/OPDn/Au CP-AFM junctions. (a) The theoretical curve (red) given by eqn (6) of the main text plotted along with the experimental curves (black) measured for different types of oligophenylene dithiol species (n=1 to 4). (b) Comparison of the theoretical (red) curve and the ensemble average (blue line) of the experimental curves. Error bars (black) represent standard statistical deviations. The number of traces as well as the minimum and maximum values of the low-bias conductance *G* are given in legends.

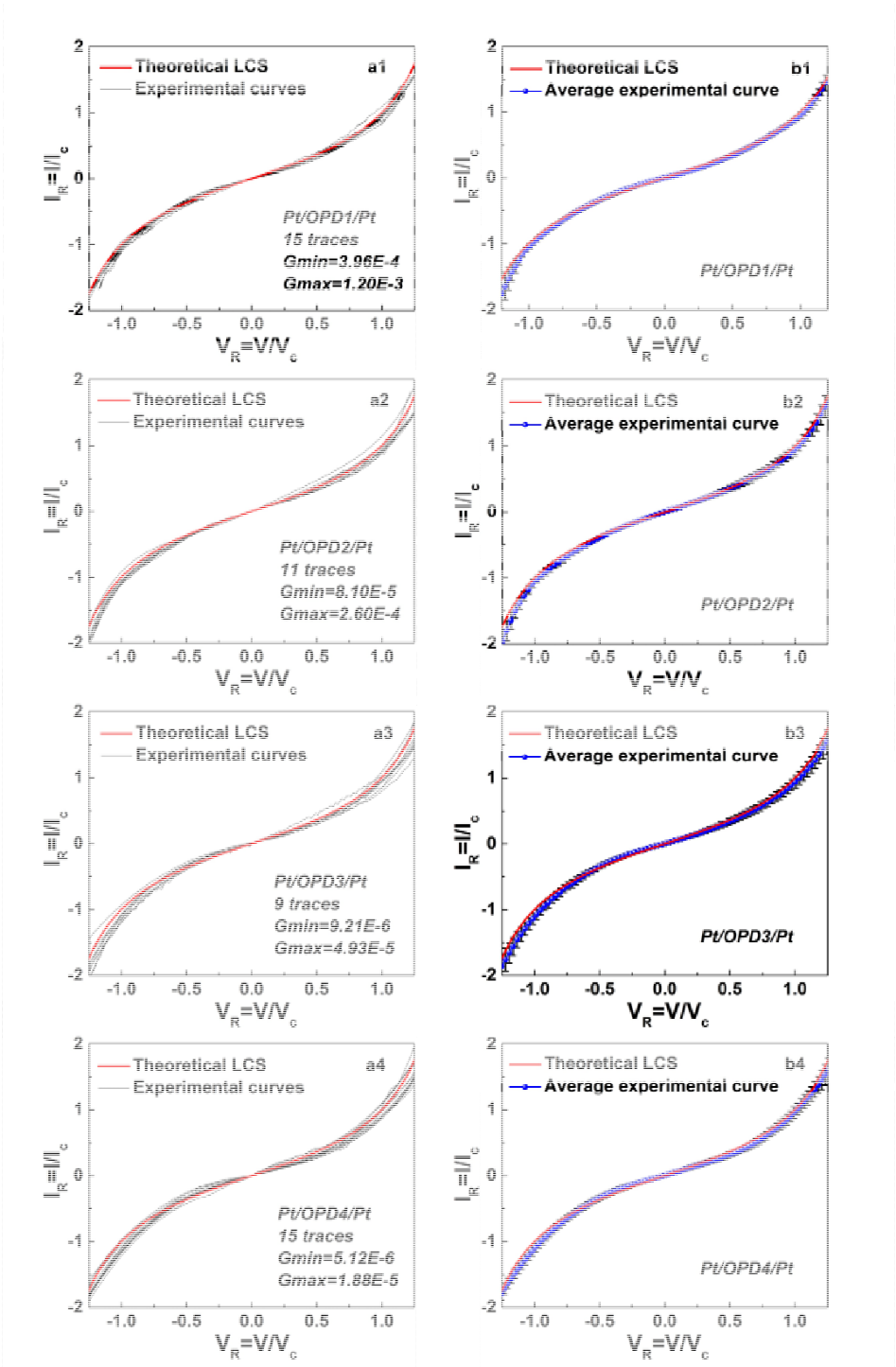

Fig. S3. Current-voltage curves in reduced variables for Pt/OPDn/Pt CP-AFM junctions. (a) The theoretical curve (red) given by eqn (6) of the main text plotted along with the experimental curves (black) measured for different types of oligophenylene dithiol species (n=1 to 4). (b) Comparison of the theoretical (red) curve and the ensemble average (blue line) of the experimental curves. Error bars (black) represent standard statistical deviations. The number of traces as well as the minimum and maximum values of the low-bias conductance *G* are given in legends.

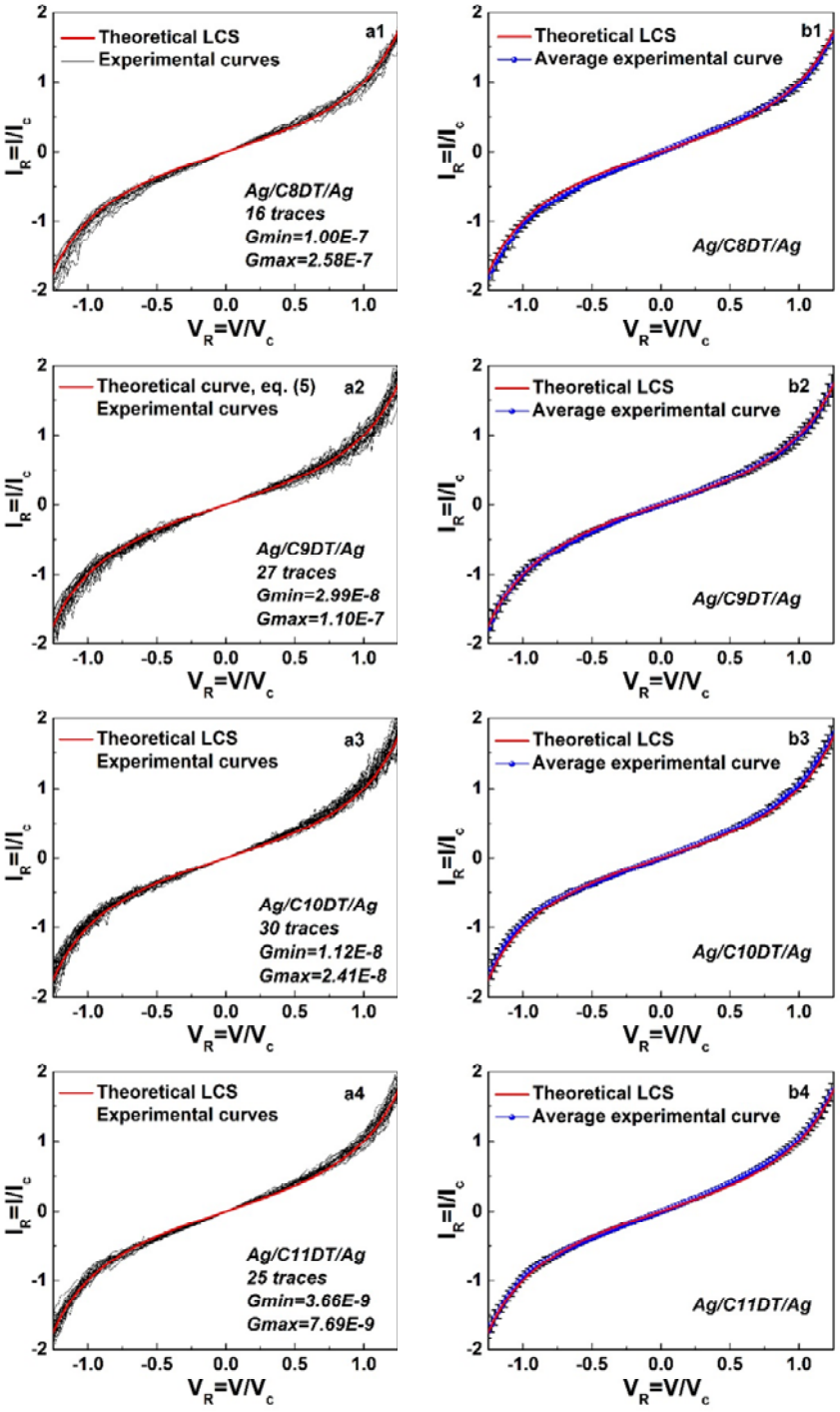

Fig. S4. Current-voltage curves in reduced variables for Ag/CnDT/Ag CP-AFM junctions. (a) The theoretical curve (red) given by eqn (6) of the main text plotted along with the experimental curves (black) measured for different types of alkanedithiol species (n=8 to 11). (b) Comparison of the theoretical (red) curve and the ensemble average (blue) of the experimental curves. Error bars (black) represent standard statistical deviations. The number of traces as well as the minimum and maximum values of the low-bias conductance *G* are given in legends.

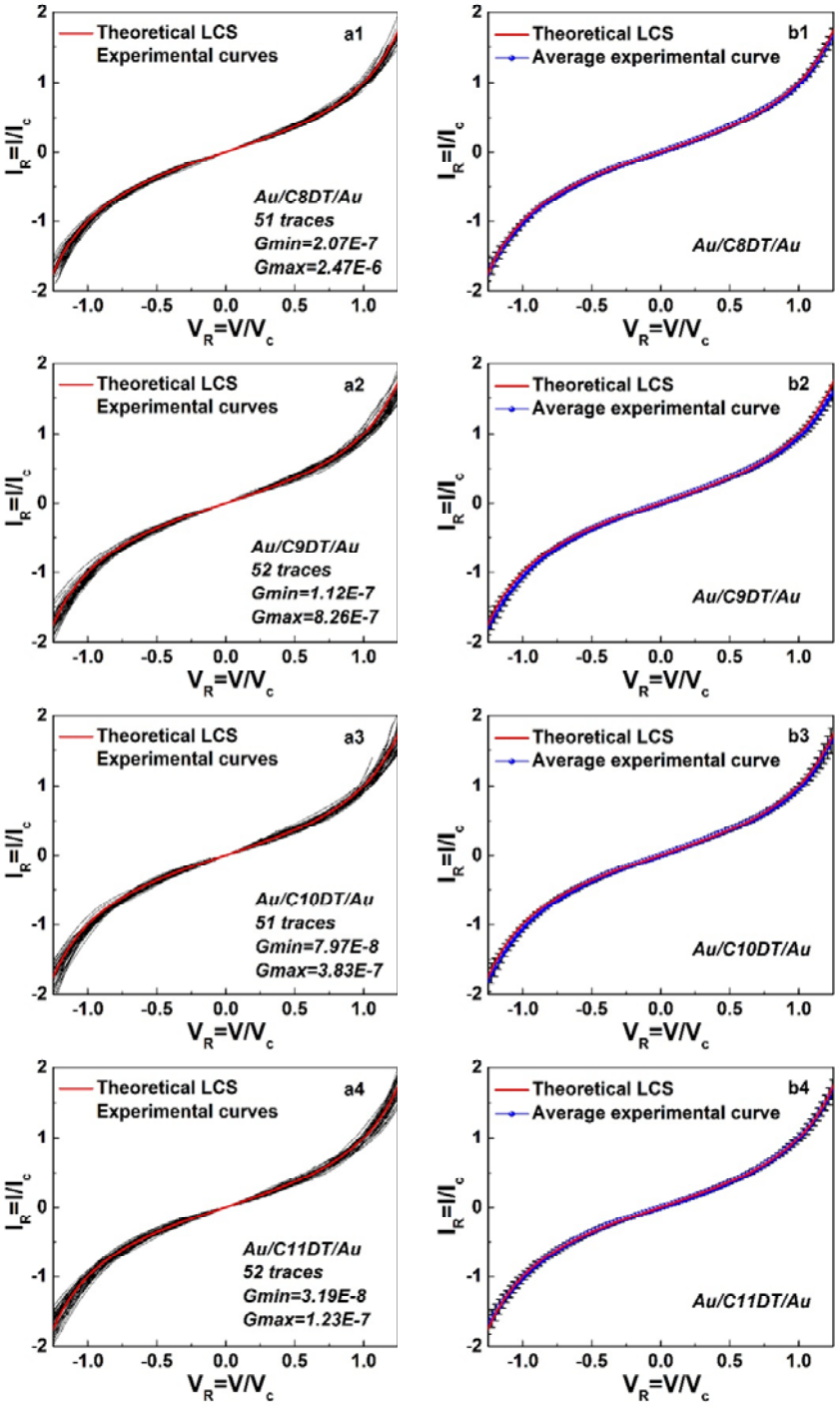

Fig. S5. Current-voltage curves in reduced variables for Au/CnDT/Au CP-AFM junctions. (a) The theoretical curve (red) given by eqn (6) plotted along with the experimental curves (black) measured for different types of alkanedithiol species (CnDT, n=8 to 11). (b) Comparison of the theoretical (red) curve and the ensemble average (blue) of the experimental curves. Error bars (black) represent standard statistical deviations. The number of traces as well as the minimum and maximum values of the low-bias conductance *G* are given in legends.

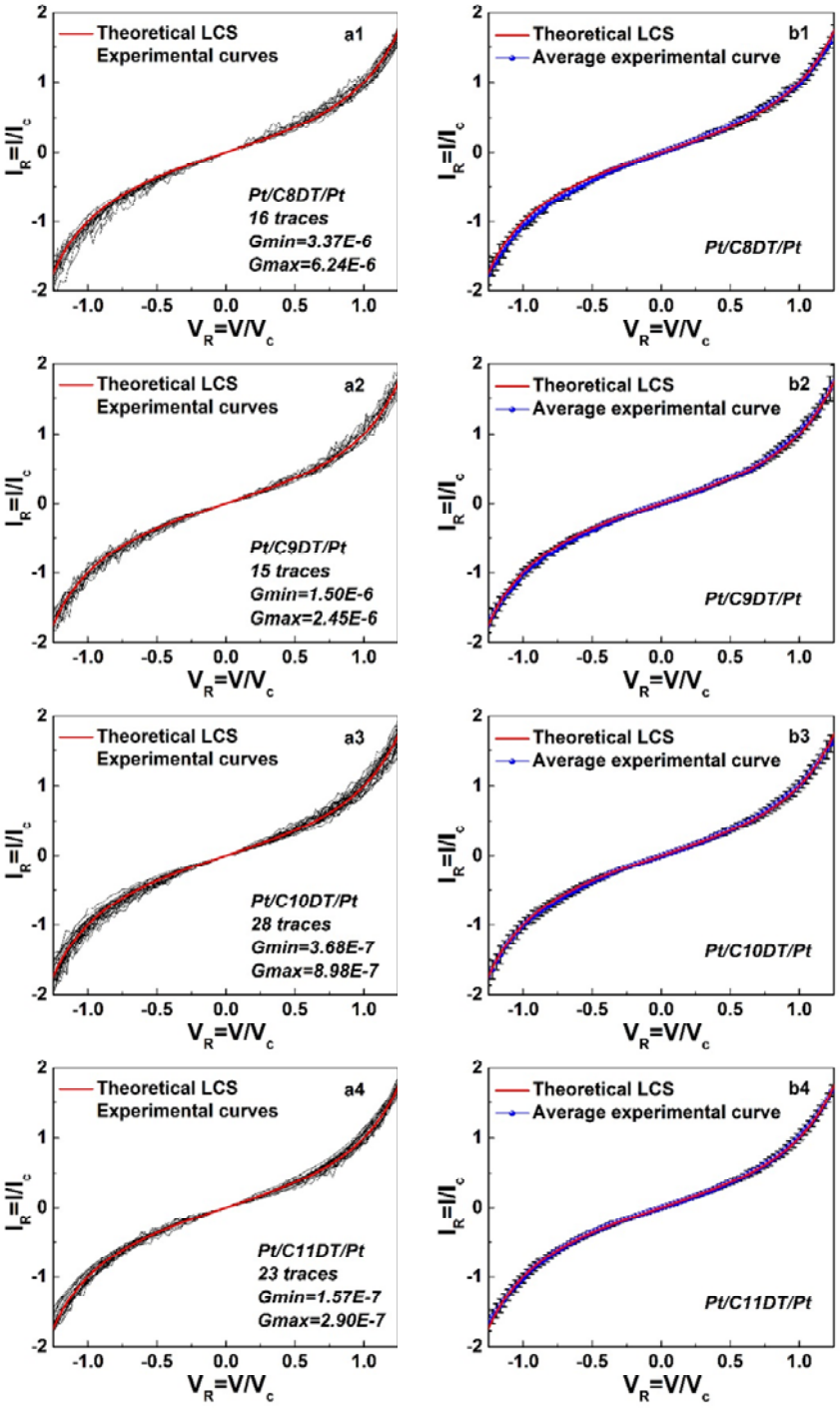

Fig. S6. Current-voltage curves in reduced variables for Pt/CnDT/Pt CP-AFM junctions. (a) The theoretical curve (red) given by eqn (6) plotted along with the experimental curves (black) measured for different types of alkanedithiol species (CnDT, n=8 to 11). (b) Comparison of the theoretical (red) curve and the ensemble average (blue) of the experimental curves. Error bars (black) represent standard statistical deviations. The number of traces as well as the minimum and maximum values of the low-bias conductance *G* are given in legends.

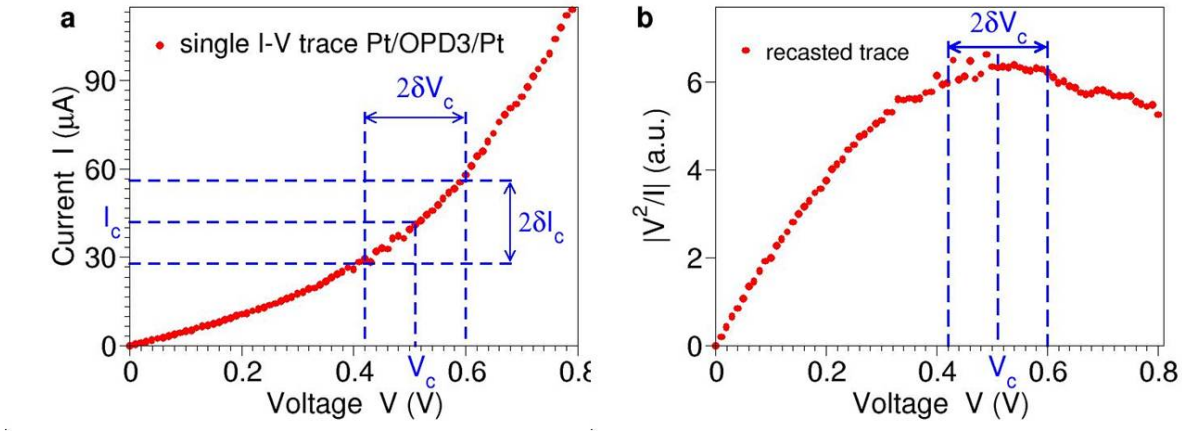

Fig. S7. Measurement errors affecting the values V_c and I_c of a single *I-V* trace. (a) A single *I-V* curve measured for a Pt/OPD3/Pt CP-AFM junction. (b) Plot of the quantity $|V^2/I|$ obtained by recasting the *I-V* trace of panel a. Inherent scattering in the measured *I-V* data yields an uncertainty in identifying the bias $V=V_c$ at the peak location (measurement error δV_c). Panel a shows how the measurement error in V_c reflects itself in a measurement error δI_c in I_c. Notice that the measurement errors (which are shown in Fig. S8 to S10) refer to a single *I-V* trace, in contrast to the statistical errors (presented in Fig. S1 to S6, and Fig. 2 and 4 of the main text), which refer to statistical ensembles comprising many traces.

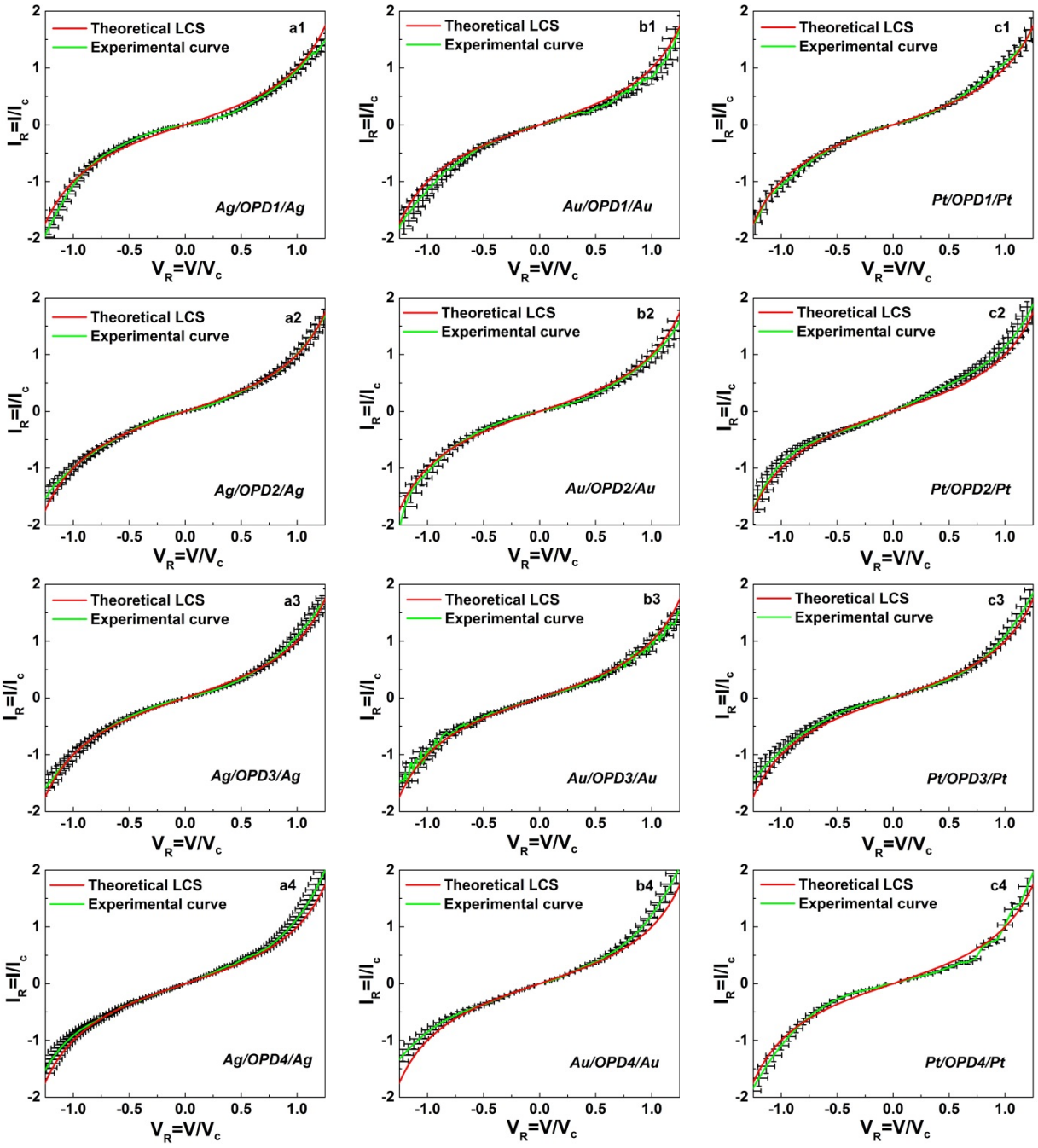

Fig. S8. Current-voltage curves in reduced variables for OPDn-based CP-AFM junctions. (a) Ag/OPDn/Ag. (b) Au/OPDn/Au. (c) Pt/OPDn/Pt. In all cases we picked out experimental traces (green) with most significant deviations from the theoretical curve (red) given by eqn (6) of the main text. The horizontal and vertical error bars, computed as $\delta V_R = |V|\,\delta V_c / V_c$ and $\delta I_R = \delta I / I_c + |I|\,\delta I_c / I_c^2$ respectively, are measurement errors (δI, δI_c and δV_c) for a *single I-V* trace; these errors should be distinguished from the statistical errors depicted in Fig. 2 and 4 of the main text and Fig. S1 to S6.

(Details on the difference between statistical errors and measurement errors are given in the caption of Fig. S7.)

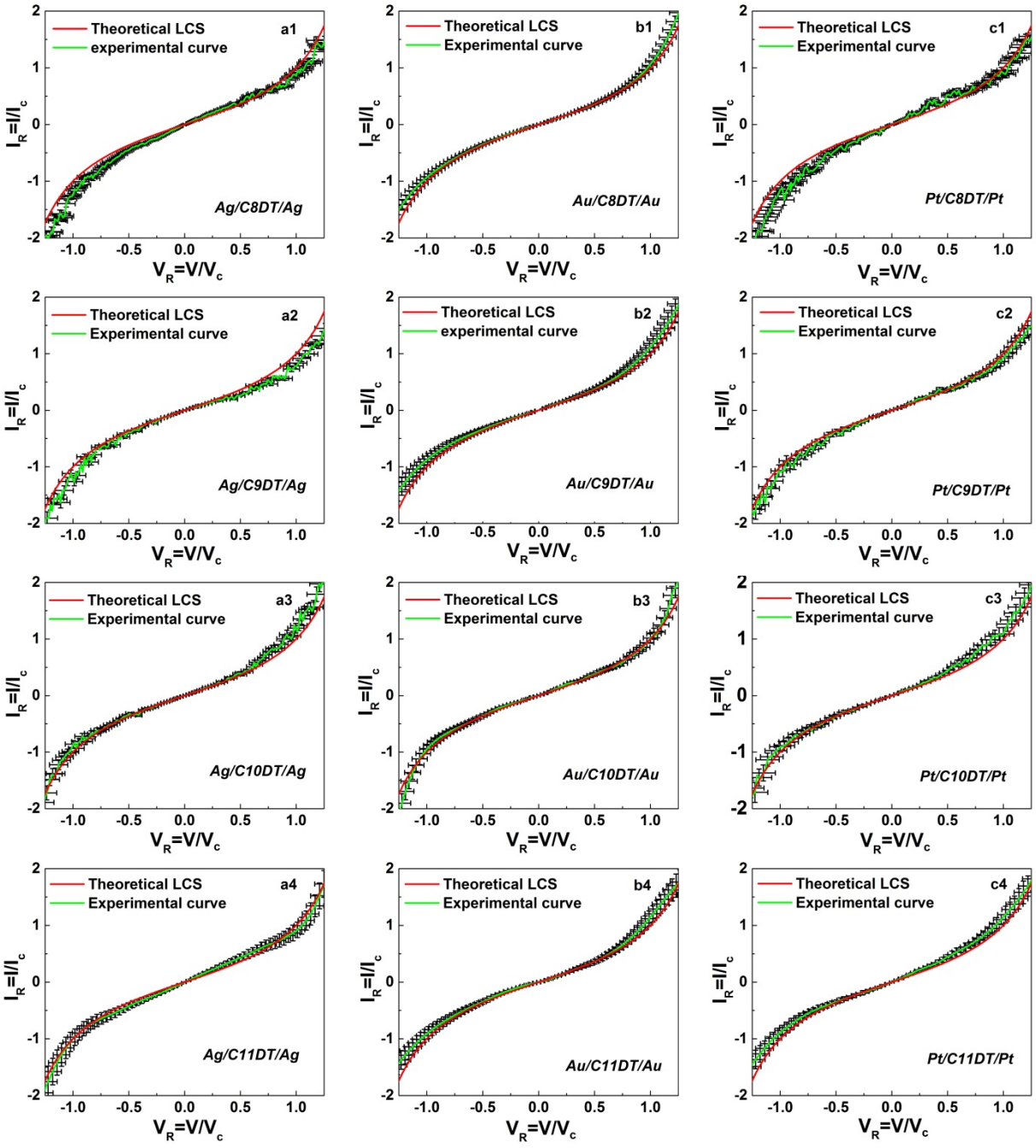

Fig. S9. Current-voltage curves in reduced variables for CnDT-based CP-AFM junctions. (a) Ag/CnDTDn/Ag. (b) Au/CnDT/Au. (c) Pt/CnDT/Pt. In all cases we picked out experimental traces (green) with most significant deviations from the theoretical curve (red) given by eqn (6) of the main text. The horizontal and vertical error bars, computed as $\delta V_R = |V|\,\delta V_c / V_c$ and $\delta I_R = \delta I / I_c + |I|\,\delta I_c / I_c^2$

respectively, are measurement errors (δI, δI_c and δV_c) for a *single I-V* trace; these errors should be distinguished from the statistical errors depicted in Fig. 2 and 4 of the main text and Fig. S1 to S6**.** (Details on the difference between statistical errors and measurement errors are given in the caption of Fig. S7.)

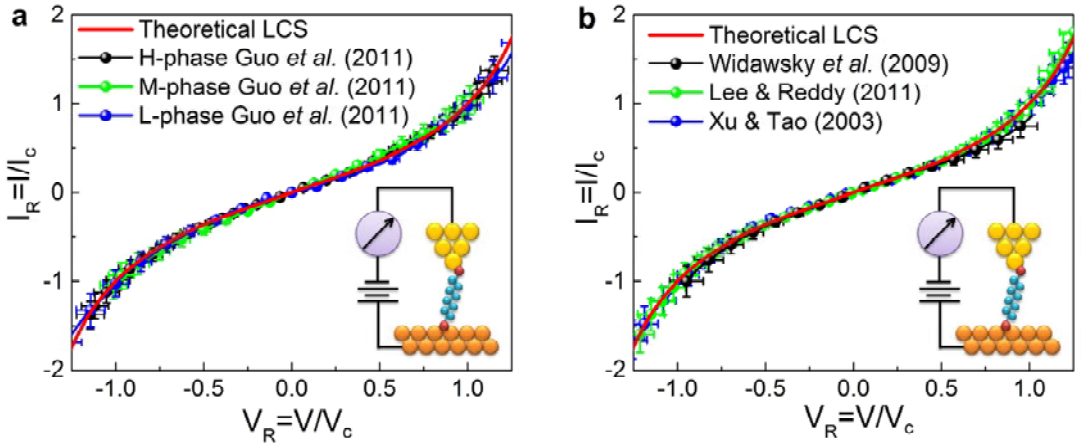

Fig. S10. The reduced current-voltage I_R-V_R traces for STM junctions of Fig. 4a and 4b from the main text are depicted here with horizontal and vertical error bars, representing "measurement errors" (cf. Fig. S7) similar to those shown in Fig. S8 and S9 for the CP-AFM junctions fabricated and measured by us.